$Ni_{59.0}Mn_{23.5}In_{17.5}$ Heusler alloy as the core of glass-coated microwires: Magnetic properties and magnetocaloric effect

V. Vega, L. González, J. García, W. O. Rosa, D. Serantes, V. M. Prida, G. Badini, R. Varga, J. J. Suñol, and B. Hernando

Citation: Journal of Applied Physics **112**, 033905 (2012); doi: 10.1063/1.4740466
View online: https://doi.org/10.1063/1.4740466
View Table of Contents: http://aip.scitation.org/toc/jap/112/3
Published by the American Institute of Physics

$Ni_{59.0}Mn_{23.5}In_{17.5}$ Heusler alloy as the core of glass-coated microwires: Magnetic properties and magnetocaloric effect

V. Vega,[1] L. González,[1] J. García,[1] W. O. Rosa,[1] D. Serantes,[1] V. M. Prida,[1,a)] G. Badini,[2] R. Varga,[3] J. J. Suñol,[4] and B. Hernando[1]
[1]*Depto. Física, Facultad de Ciencias, Universidad de Oviedo, Calvo Sotelo s/n, 33007 Oviedo, Spain*
[2]*Instituto de Ciencia de Materiales de Madrid (CSIC), Campus de Cantoblanco, 28049 Madrid, Spain*
[3]*Institute of Physics, Faculty of Science, UPJS, 041 54 Kosice, Slovakia*
[4]*Universidad de Girona, Campus de Montilivi, edifici PII. Lluís Santaló s/n, 17003 Girona, Spain*

(Received 8 April 2012; accepted 5 July 2012; published online 2 August 2012)

Heusler $Ni_{59.0}Mn_{23.5}In_{17.5}$ alloy was prepared as the metallic core of a glass-coated microwire with a total diameter of 41.8 μm. X-ray diffractograms performed at room temperature and 100 K show a highly ordered $L2_1$ cubic structure characteristic of the austenitic phase in Heusler alloys. Thermomagnetic curves measured in the temperature range from 50 K up to 400 K show ferromagnetic coupling in the austenite with the Curie temperature around 246 K. Hysteresis loops measured at different temperatures indicate a soft ferromagnetic behaviour, confirming the microwire axis as the magnetization easy direction. The magnetic entropy variation reaches a maximum value of 1.75 J/kgK at the ferro-to-paramagnetic phase transition for a magnetic field change of 30 kOe. After short annealing, the Curie temperature is almost unchanged while the maximum entropy change increases up to 2.01 J/kgK. Refrigerant capacity and its dependence on both working temperature range and applied field value are evaluated for all microwire samples, reaching 120 J/kg for a 30 kOe magnetic field variation. We analyze the possibility of employing microwire shape Heusler alloys as low field magnetocaloric micro-devices and solid-state actuators. © *2012 American Institute of Physics*. [http://dx.doi.org/10.1063/1.4740466]

I. INTRODUCTION

Thin microwires are suitable materials for many technological applications due to their outstanding properties, such as magnetic bistability,[1] magneto-optical, and tunable microwave absorption properties,[2,3] chemical sensing,[4] superelasticity,[5] and high frequency behaviour.[6] The great attention recently paid in glass-covered microwires derives from their reduced dimensionality, composite nature, and proposed use as novel functional materials.[7] The well-controlled geometry of these thin microwires is obtained through the fast-solidification Taylor-Ulitovsky method.[8] This technique allows the fabrication of cylindrical composites of glass-coated metallic alloys with a typical nucleus diameter ranging from 1 to 30 μm. The glass-coating thickness varies between 0.5 and 20 μm owing to the high enough quenching rate process.[8] The glass-cover yields an improvement in the mechanical properties of these composites, inducing in the metallic core strong residual stresses arising from their difference in thermal expansion coefficients.[8]

Fast-solidifying techniques have been proved as cost-effective to fabricate some wire-shape ferromagnetic materials with granular structure, exhibiting high-magnetostrictive and magnetocaloric effects.[9,10] Heusler alloy wires with ferromagnetic shape memory effect[11–15] have also been obtained, where martensitic transformation is triggered not only by changes in temperature and/or stress but also by changes in the applied magnetic field.[16] These micromaterials can be proposed for its use in magneto-mechanical actuators based in shape memory effect, spintronics, and magnetocaloric devices for environmentally friendly magnetic refrigeration.[9–16] All these applications require ferromagnetic materials displaying large changes in such magnetic properties related to first order magnetostructural transformations and/or second order magnetic transitions around room temperature (RT). Among them, Ni-Mn-X (X = Ga, Sn, In, etc.) Heusler alloys undergo a martensitic transformation exhibiting multifunctional properties as shape-memory effect,[17] large inverse magnetocaloric effect[18] and magnetic superelasticity,[19] magnetoresistance effect and exchange bias behavior.[20–23] Recently, Mañosa *et al.* have studied the influence of hydrostatic pressure on the magnetic and structural properties of Ni-Mn-In shape-memory alloys[24] and found a large barocaloric effect as a consequence of the volume and entropy discontinuities at the magnetostructural transition.[25] Most of these properties are critically dependent on the austenite to martensite phase transition occurring in magnetic shape memory alloys at a certain temperature strongly dependent on the chemical composition of the sample.[26–30] The usage of magnetocaloric micromaterials in the form of thin films, ribbons, or microwires in the manufacture of refrigerators can optimize the heat transfer between the working body and the heat exchange fluid in comparison with bulk samples, thus improving the technical characteristics of refrigeration unit.[31] Both, microwire shape and glass-coating mechanical reinforcement are very interesting features, not only for investigation of these effects on such kind of alloys but also for their applications as magneto-mechanical sensors

a)Author to whom correspondence should be addressed. Electronic mail: vmpp@uniovi.es.

and may significantly influence the microwire magnetic behavior.[32] This shape is also suitable for the development of composite materials, i.e., embedding them in a polymeric matrix.[33]

For the present work, a Ni-Mn-In Heusler alloy with an off-stoichiometric composition has been prepared as the core of a glass-coated microwire. We have studied the sample microstructure, magnetic, and magnetocaloric properties in the temperature range from 50 K up to 400 K. In this temperature interval, a soft magnetic behaviour was observed in agreement with the high symmetry $L2_1$ cubic crystalline structure checked by x-ray diffraction (XRD) performed at different temperatures. However, no martensitic transformation was reached, thus the magnetic entropy change is uniquely due to a ferro-to-paramagnetic phase transition, and then a negative variation occurs with a maximum near the Curie temperature, T_C. Influence of short annealing on magnetic and magnetocaloric properties of the Ni-Mn-In microwires is also discussed. The refrigerant capacity and its dependence on the range of the working temperature interval and applied magnetic field are evaluated and compared for microwires in the as-quenched state and after thermal annealing. We obtain a noticeable magnetocaloric effect and significant refrigerant capacity values, as compared to Ni-Mn-In alloy ribbons with similar compositions,[28,29,31] revealing Heusler alloy microwires very promising for multifunctional applications.

II. EXPERIMENTAL DETAILS

A Heusler $Ni_{50}Mn_{34}In_{16}$ master alloy was obtained after arc-melting highly pure elements (99.999%) in Ar atmosphere. Ingots were melted several times to ensure a good starting homogeneity. Further, ferromagnetic microwires with $Ni_{59.0}Mn_{23.5}In_{17.5}$ chemical composition, having an inner metallic core diameter around 19.3 μm and a glass-coating outer shell diameter about 41.8 μm, were obtained by the Taylor–Ulitovsky technique,[8,34] as shown in Fig. 1(a). Thus, when the metallic alloy and the Pyrex glass coating were simultaneously molten, the so-formed microwire was drawn and rolled onto a rotating coil and quenched to room temperature. Materials thus obtained were in the form of a tiny glass-coated metallic wire with the dimensions above mentioned. Some of the as-quenched microwires were subsequently annealed at 473 K and 498 K in a protective Ar atmosphere for 10 min. After that, they were slowly cooled down to room temperature, in order to relax internal stresses and achieve ferromagnetic ordering with Curie temperature near room temperature.

Scanning electron microscopy (SEM) with energy dispersive x-ray spectroscopy microanalysis (EDS) was used to perform a morphological characterization and elemental composition analysis in all studied samples. X-ray diffraction patterns were analyzed at 100 K and 300 K using CuK_α radiation in a low-temperature diffractometer with a 0.05° step increment. A VSM Versalab magnetometer (Quantum Design) was employed for measuring zero-field cooling, field-cooling, and field-heating (ZFC–FC–FH) magnetization vs. temperature curves in the range from 400 K down to 50 K and at different

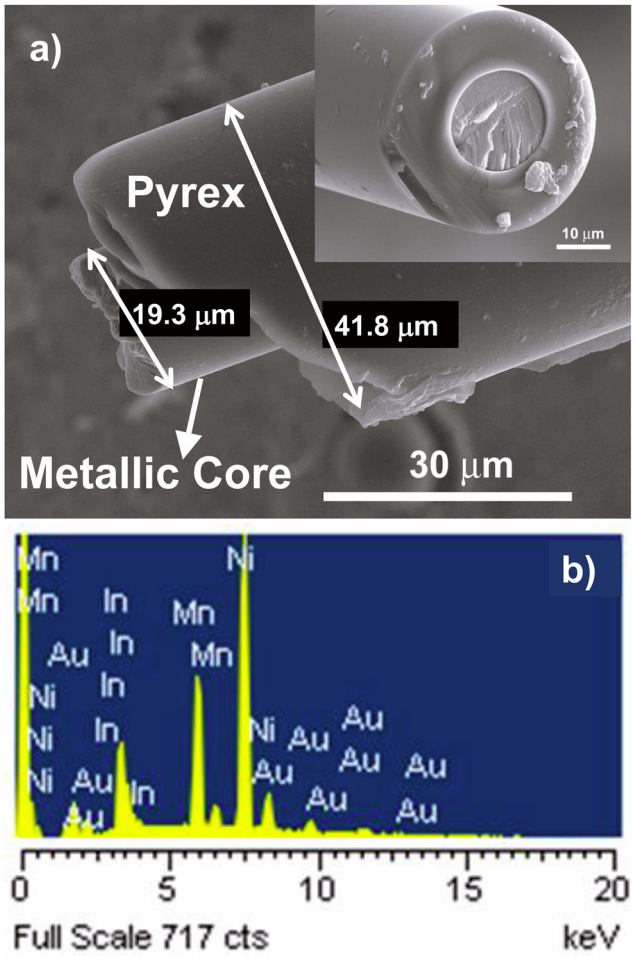

FIG. 1. (a) SEM images at different magnifications of as-quenched Ni-Mn-In microwire fracture cross-section of both metallic nucleus and Pyrex glass coating and (b) EDS microanalysis. Gold presence is due to its evaporation on the sample surface for enhancing the electrical conductivity.

applied magnetic field values from 1 kOe up to 30 kOe. The field was applied along the microwire axis for studying the magnetization dependence of the temperature. Hysteresis loops were measured up to 10 kOe applying the field parallel and transversely to the wire axis using a superconducting quantum interference device (SQUID) magnetometer.

III. RESULTS AND DISCUSSIONS

A. Microstructural characterization

Fig. 1(a) shows SEM images at different magnifications of as-quenched Ni-Mn-In microwires fracture cross-section and diameter dimensions of both, metallic core and Pyrex glass coating. From the direct checking of the inner metallic nucleus, no ordered microstructure can be detected, suggesting that the heat removal during the rapid solidification process does not induce any directional growth in the formed crystalline phase. After a systematic study made by EDS microanalysis on the fractured cross-section surface of microwires, by testing an appreciable number of sample pieces, a nearly homogeneous chemical elements distribution was shown with an averaged composition about $Ni_{59.0}Mn_{23.5}In_{17.5}$. For instance, an EDS pattern for the as-quenched

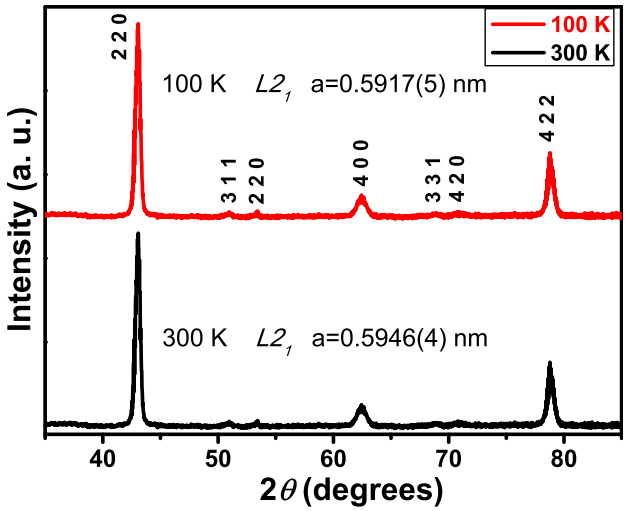

FIG. 2. XRD at 300 K (bottom) and 100 K (top) of the as-quenched $Ni_{59.0}Mn_{23.5}In_{17.5}$ microwire.

microwire can be seen in Fig. 1(b). The gold presence is due to its evaporation on the sample for enhancing its electrical conductivity and improvement of the SEM image contrast. The estimated error in determining the concentration of each element was of ±0.1%. None appreciable contamination with silicon impurity was observed. The Mn deficiency with respect to the alloy nominal composition could be due to its evaporation during the melting process.

The crystalline structure of $Ni_{59.0}Mn_{23.5}In_{17.5}$ microwire was checked by XRD at RT and 100 K by using the WINPLOTR program (FULLPROF software packet) (Ref. 35) to identify its symmetry and calculate the lattice parameters. Both diffraction patterns are shown in Fig. 2. All identified peaks correspond to a highly ordered $L2_1$ cubic structure characteristic of the austenite phase in Heusler alloys, probably with part of the Ni atoms placed in several typical sites of Mn and In atoms because of the off-stoichiometry composition. The same behavior was found in other non-stoichiometric Ni-Mn-In Heusler alloys.[36,37] The existence of peaks associated to the reflections indexed as (311) and (331) confirms the $L2_1$ phase at both RT and 100 K. Furthermore, XRD peaks are similar in their relative intensities at both temperatures, indicating the same texture. The lattice parameter a = 0.5946(4) nm associated to RT exhibits just a slight decreasing down to a = 0.5917(5) nm at 100 K. This deviation in lattice parameters could be partially attributed to the high levels of stress originating from the difference between the thermal expansion coefficients of the metallic core and the glass coating.[14]

B. Magnetic hysteresis loops

Magnetization response to the magnetic field of the as-quenched Ni-Mn-In microwire was measured by applying the field either parallel and/or perpendicular to the microwire axis. Figs. 3(a) and 3(b) display hysteresis loops performed at 300 K and 100 K for a maximum applied field of 10 kOe, respectively, and Figs. 3(c) and 3(d) show a zoom of both loops in the low field range. The diamagnetic contribution of the glass coating has been directly subtracted from the measurements. Clear ferromagnetic behavior is observed at 100 K with a steep rise of magnetization at low applied field and a tendency to saturation at higher fields. The coercive field is found to be small, around 76 Oe, signifying the soft ferromagnetic character of the sample due to its low magnetocrystalline anisotropy, as a consequence of the high cubic symmetry of austenite, along with shape and magnetoelastic anisotropies. Comparing the loops measured in both directions, it is clear that the easy axis lies parallel to the microwire axis. In fact, the hysteresis loop measured when the field is applied in the transverse direction to the microwire axis shows a gradual increase in the magnetization up to a highest field value for reaching the saturation, which

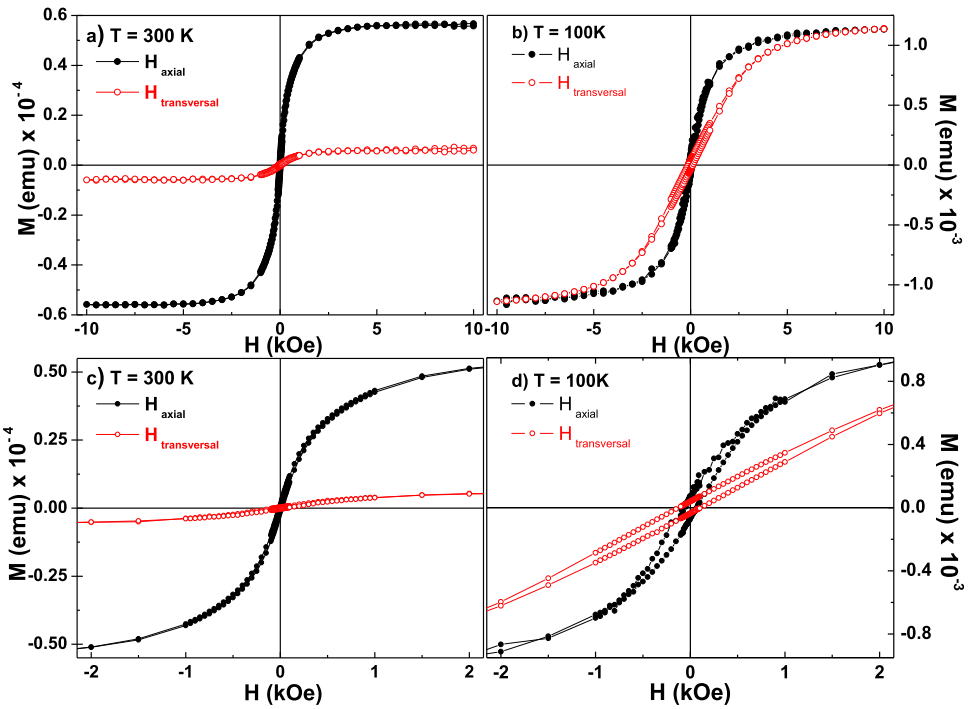

FIG. 3. (a) and (b) Hysteresis loops performed at 300 K and 100 K, respectively, for magnetic field applied parallel to the as-quenched $Ni_{59}Mn_{23.5}In_{17.5}$ microwire axis (H axial) and perpendicular to it (H transversal); (c) and (d) zoom of above mentioned hysteresis loops up to $H = 2$ kOe at 300 K and 100 K, respectively.

confirms that direction as the magnetization hard axis. This behavior is supported by the predominance of shape anisotropy and the strong axial stresses that deform the crystalline lattice in the same direction.

Being T_C around 246 K, at 300 K, we find a decrease of magnetization in two orders of magnitude and a coercivity around 10 Oe, related to the ferromagnetic-paramagnetic phase transition but with some residual ferromagnetic phase still present as derived from the shape of the hysteresis loop.

C. Thermomagnetic and isothermal characterization

Figs. 4(a)–4(c) show ZFC-FC-FH thermomagnetic curves for as-quenched and annealed microwires at 473 K and 498 K. Different magnetic field values ranging from 1 kOe up to 20 kOe were applied in the temperature range from 50 K up to 400 K. The $M(T)$ behavior corresponds to a typical ferromagnet for applied fields equal and higher than 5 kOe. At high temperatures, the material becomes paramagnetic and orders ferromagnetically below $T_C \approx 246$ K. It can be observed that FH data do not retrace the FC data but show a thermal hysteresis. This feature can be better observed in the inset of Fig. 4(a), where a magnification of the $M(T)_H$ curves for the as-quenched microwire has been performed in the temperature interval between 190 K and 280 K. This thermal hysteresis decreases with the increasing applied field suggesting that it could be suppressed when higher magnetic fields than 30 kOe were applied. This magnetic phase transition cannot be associated to any thermally induced structural transformation of the microwire because crystalline phases detected at RT and 100 K are both equal and similar in their relative intensity, retaining the cubic $L2_1$ structure. The origin of this thermomagnetic behaviour could lie in the thermal lag between the metallic core temperature and the recorded temperature through the glass coating. In the case of the as-quenched microwire and the one annealed at 498 K, the low-temperature $M(T)$ at H = 1 kOe exhibits a separation between ZFC and FC curves, which tends to disappear in higher magnetic fields. This splitting could be due to some weak antiferromagnetic (AFM) exchange introduced by Mn-Mn neighbours with smaller separation than in the stoichiometric alloy. It must be remarked that in our off-stoichiometric Ni-Mn-In alloy, the rapid quenching might increase the site disorder of atoms occupation leading to Mn-Mn AFM coupling. This AFM exchange can pin ferromagnetic domains if the sample is cooled through in a small applied field leading to the separation between ZFC and FC curves. This behavior has also been observed in other Ni-Mn-In Heusler alloys without any signature of martensitic transformation,[35] as it happens for the sample here reported. In all cases, we find a decrease of magnetization when increasing the applied field. It arises from the Pyrex diamagnetic contribution with negative signal, leading to negative magnetization values at temperatures above the FM-PM transition. $M(T)$ curves measured at ZFC-FC-FH regimes for microwires annealed at 473 K and 498 K are shown in Figs. 4(b) and 4(c), respectively. It was found that with increasing temperature, the FM-PM transition takes place at around 247 K and 248 K as it can be observed in their corresponding ZFC curves at 1 kOe. $M(T)$ behavior is

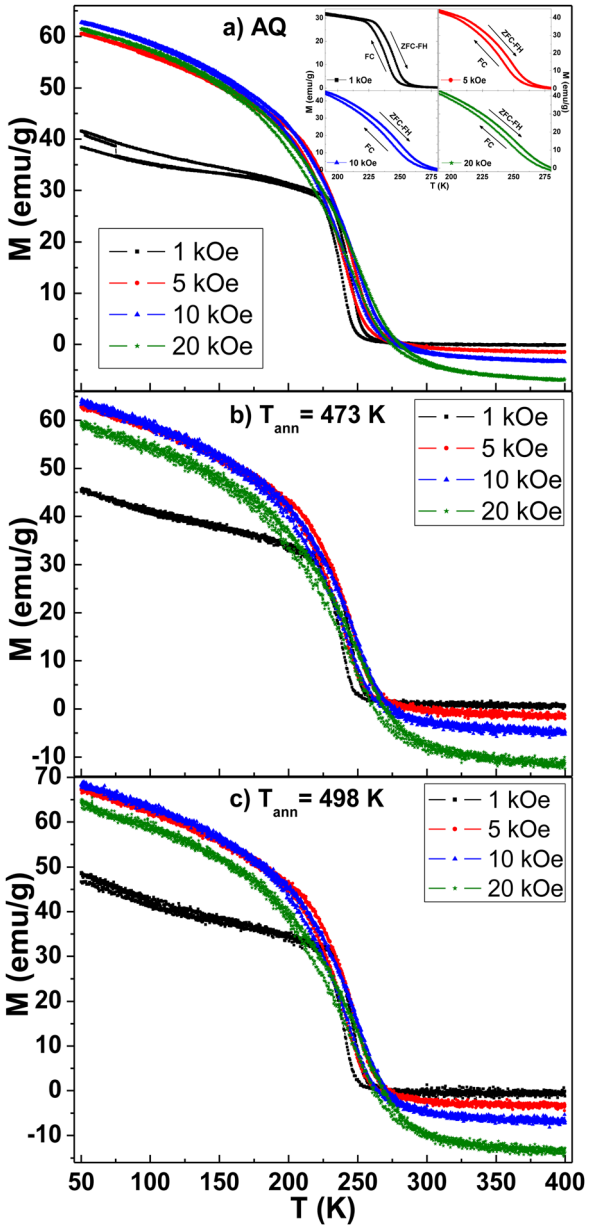

FIG. 4. ZFC, FC, and FH, $M(T)$ curves measured in the temperature interval of 50 K $\leq T \leq$ 400 K under different applied axial field H values from 1 kOe up to 20 kOe for (a) as-quenched $Ni_{59.0}Mn_{23.5}In_{17.5}$ microwire; (b) microwire annealed at 473 K; and (c) microwire annealed at 498 K. The inset of Fig. 4(a) shows a magnification of $M(T)_H$ curves in the temperature interval between 190 K and 280 K.

quite similar in both annealed samples in comparison with the as-quenched microwire, and FC curves retrace ZFC curves out of the temperature interval when the FM-PM transition occurs.

The Curie temperature is almost unchanged for both annealed microwires, but a slight increase of the magnetic moment at low temperature is observed, being higher for the microwire annealed at 498 K. The splitting between ZFC and FC curves at low temperature is also present in annealed samples, although is somewhat reduced at 1 kOe but clearly appears at 20 kOe for the microwire annealed at 498 K. These minor variations can be ascribed to the influence of the annealing process even at the low temperatures here employed. After the heat treatment, microwires probably

undergo a grain size growth favored by structural relaxation as can be observed in melt spun ribbons of similar Ni-Mn-In alloys composition by SEM[38] as well as in glass coated Fe-rich microwires by XRD.[39] This effect may slightly modify the inter-atomic distances, changing the atomic order-disorder degree and leading to a Mn-Mn separation that would be short enough so that an AFM exchange of substantial strength can be maintained even at an applied field value of 20 kOe (see Fig. 4) and even up to 30 kOe.

Additional information on the nature of the phase transition can be obtained from the Arrott plots shown in Figs. 5(a) and 5(b), after transferring the *M-H* isotherms measured along the parallel to the wires axis (a) and perpendicular ones (b) (see the respective insets) into M^2 vs. H/M plots. This method provides a criterion to identify whether the transitions observed are of first-order or second-order nature. The S-shape negative slope of the M^2 vs. H/M plots is indicative of a first-order character of the magnetic transformation. It is worth noting that the curvature in the M^2 vs. H/M curves is positive for nearly all temperatures around $T_C = 246$ K. Therefore, the nature of the magnetic phase transition at T_C could be of second order.[40] This second-order behaviour of the Arrott plots at the FM-PM transition is also confirmed by the absence of hysteresis losses in the isothermal $M(H)$ curves, in spite of the thermal hysteresis observed in $M(T)$ measurements. Thus, these arguments further support our criterion that the origin of the thermal hysteresis in the $M(T)$ curves lies in the existence of a lag between the temperature of the magnetic core and the recorded temperature during the measurement, due to the surrounding glass thickness with different thermal conductivity.

IV. MAGNETOCALORIC EFFECT

A. Magnetic entropy change

The magnetic field-induced entropy change, ΔS_M, was computed from ZFC magnetization measurements for the as-quenched and annealed microwires, as a function of the temperature and applied magnetic field, by using the Maxwell relation $\Delta S_M(T,H) = \mu_0 \int_0^H \left(\frac{\partial M}{\partial T}\right)_{H'} dH'$.[29] Results are collected in Fig. 6(a) for applied field values up to 30 kOe. In the temperature range between 100 and 350 K, $(\partial M/\partial T)_H$ is negative (see Fig. 4) for all samples. Thus, a conventional magnetocaloric effect is observed around T_C in this temperature range near the FM-PM transition as a negative entropy change. A maximum entropy variation around 1.75 J/kgK is achieved for a magnetic field change value of 30 kOe, almost the same value for both the as-quenched microwire and the one annealed at 473 K. Meanwhile, the larger value of maximum ΔS_M reaches about 2.01 J/kgK for the microwire annealed at 498 K that can be related to the abrupt change in the magnetization and larger values of ΔM at T_C. All these ΔS_M maxima values are well above the ones obtained for other microwire samples[9,14] and comparable to that found in

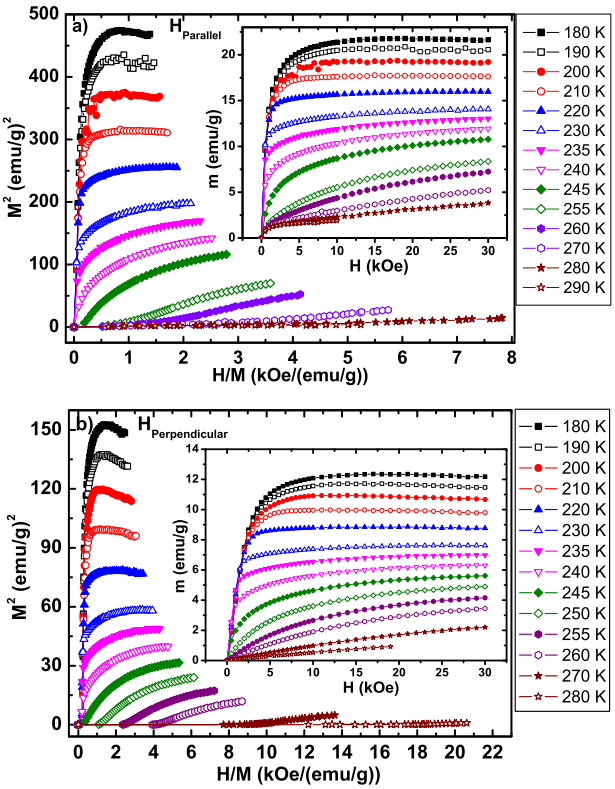

FIG. 5. M^2 vs. H/M Arrott plots computed from the *M-H* isotherms measured for the as-quenched $Ni_{59.0}Mn_{23.5}In_{17.5}$ microwire along (a) parallel to the wire axis and (b) perpendicular one. The respective insets display both parallel and perpendicular *M-H* isotherms measured in the temperature interval around T_C.

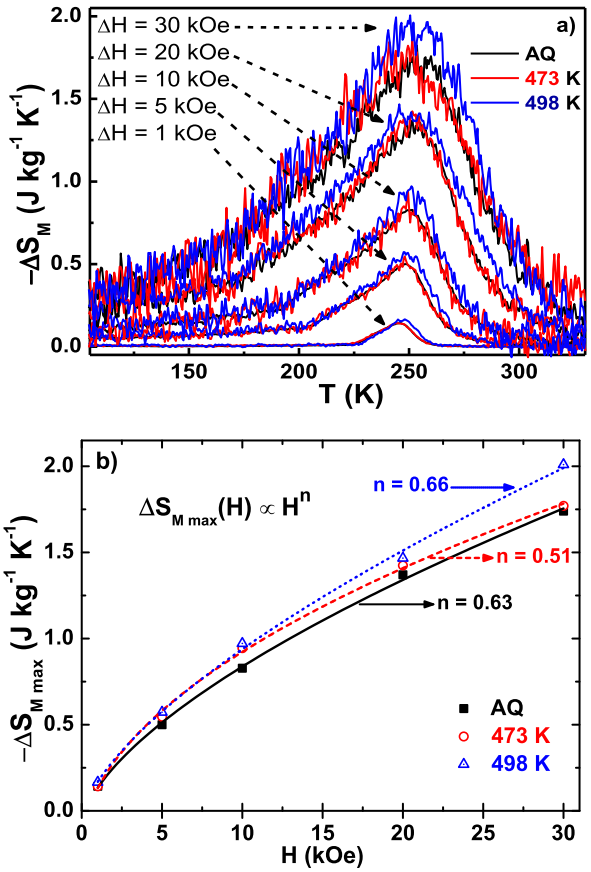

FIG. 6. (a) Entropy change as a function of temperature measured around the paramagnetic-ferromagnetic transition for as-quenched an annealed $Ni_{59.0}Mn_{23.5}In_{17.5}$ microwires at 473 K and 498 K, plotted for selected magnetic field values and (b) maximum of the magnetic entropy change for the three same samples at selected field values.

ribbons of similar composition showing a magnetic phase transition.[29,31]

At a certain temperature at which the magnetic entropy change peaks its maximum value ($\Delta S_{Mmax.}$), the $\Delta S_{Mmax.}$(H) field dependence follows the power law $\Delta S_{Mmax.} \propto H^n$, where the exponent n depends on the magnetic state of the sample and can be locally calculated as $n = d\ln|\Delta S_M|/d\ln H$.[41] As it is shown in Fig. 6(b), the field dependence of the maximum of the magnetic entropy change at the temperature of the peak fits to a field independent exponent of $n = 0.63$, 0.51, and 0.66, for the as-quenched microwire and the ones annealed at 473 K and 498 K, respectively. These n values are relatively close to the 2/3 value corresponding to a mean field model.[42,43]

B. Refrigerant capacity analysis

In addition to the magnetic entropy change analysis, we have also performed a detailed study of the so-called refrigerant capacity (*RC*) on the samples. The *RC* provides an estimation of the amount of heat that can be removed in one thermodynamic process in this temperature interval. It can be defined as the area comprised below the ΔS_M curve in a certain interval taken as the temperature width at half maximum (TWHM), given by $RC = \int_{T_{cold}}^{T_{hot}} [\Delta S_M(T')]_{\Delta H} dT'$, where T_{cold} and T_{hot} are the temperature of the cold and hot sinks, respectively.[29] Although this amount will be obviously proportional to the height of the ΔS_M curve, also its shape must be taken into account. A material exhibiting only a very large but too narrow ΔS_M peak would not be adequate for refrigeration purposes. Therefore, *RC* is a key parameter from the application point of view, since for refrigeration purposes the important property is not only how large the entropy change can be at a given temperature but rather the amount of heat that can be released in a given thermodynamic cycle (for example during adiabatic demagnetization in a Brayton cycle). *RC* values as a function of the magnetic field for all samples considered are shown in the top row of Figs. 7(a)–7(c), where the as-quenched (a) and annealed microwires (b) and (c) exhibit a similar dependence on the applied magnetic field. The three samples display a monotonous increase of the *RC* with values around 80 J/kg for a field value of 20 kOe (typical static field value that can be currently generated without energy cost employing permanent magnets) and higher than 120 J/kg at 30 kOe, which are comparable to (or even larger than) values obtained in other Heusler type magnetocaloric materials with similar compositions[29,31] and geometry.[9,14]

The proper definition of *RC* value above described implies that very broad curves could stand for very high *RC* values even for relatively small ΔS_M values.[29,31] This could induce to misleading interpretations about the quality of a given material for refrigeration purposes, since high *RC* values arising from too flat entropy curves would imply very large values of the working temperature range (*WTR*) between hot and cold reservoirs, $WTR = T_{hot} - T_{cold}$. However, for practical applications, the desirable *WTR* is often limited to be of the order of tens of degrees, and hence from this point of view, a material must simultaneously fulfill both requirements: large ΔS_M and suitable FWHM according with the *WTR*.

A more realistic alternative could be to evaluate *RC* in the specific *WTR* required for a particular application, so that a systematic comparison of different magnetocaloric materials can be performed.[44] For such a purpose, we have also computed the *RC* for some different *WTR* values (10 K, 20 K, and 40 K). These results are plotted in (a)-(c) upper row of Fig. 7, where a decrease of *RC* is observed while

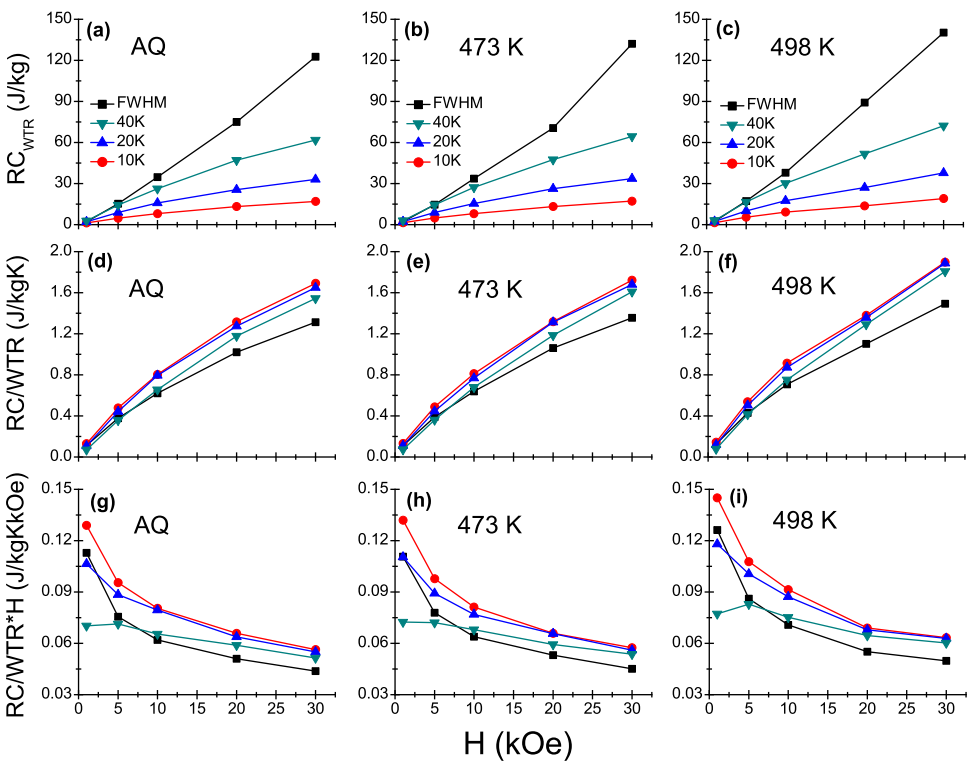

FIG. 7. (a)–(c) *RC* evaluated at some different *WTR* intervals for as-quenched an annealed $Ni_{59.0}Mn_{23.5}In_{17.5}$ microwires at 473 K and 498 K; (d)–(f) normalized *RC/WTR* plots; and (g)–(i) field normalized *RC/WTR* curves, for the three same samples.

lowering the *WTR*. The field dependence of *RC* evaluated in this way behaves also linearly for the different *WTR* values considered. However, if we want to assess the relative effectiveness of the *RC* for different *WTR* values, it is necessary to weight each *RC* value by the corresponding *WTR*. This will provide us with a detailed description of the performance of the material for a certain *WTR* (refrigeration capacity per K degree). Normalized *RC/WTR* data are displayed in the middle row of Figs. 7(d)–7(f). It is observed that the higher *RC/WTR* is obtained for the smaller *WTR*. This feature becomes evident if we realize that the smaller the *WTR*, the more close we are to the maximum, where the curve is more flat and so the values are larger. What is important from these results is that they provide a measure of the performance of the material, indicating how it diminishes depending on the desired *WTR*. For example, for the as-quenched microwire, if operating at a 20 kOe field, it is observed a drop in the *RC/WTR* of 11% when the *WTR* varies from 10 K to 40 K, and of 23% when it changes from 10 K to FWHM. The thermal treatment of the microwires results in a 2% and 4% improvement for the samples annealed at 473 K and 498 K, respectively.

Further on, in order to assess the optimizing operating conditions for magnetocaloric applications of the NiMnIn Heusler microwire, we have specifically weighted the *RC/WTR* value also by the magnetic field strength. We have previously found the existence of an optimizing value of the applied field for magnetocaloric applications in highly anisotropic systems with cylindrical symmetry as nanoparticle chains and nanowires.[45] In order to check out if such a behavior is reproducible in our Ni-Mn-In magnetic microwires, the field weighted values of *RC/WTR* are shown in the lower row of Figs. 7(g)–7(i). The main feature that can be observed is that the values of the normalized field *RC/WTR* are in general larger for small *WTR* values and they decrease with the applied field. However, a striking feature is observed in the case of $WTR = 40$ K curve at low magnetic fields, where a well-defined maximum appears at 5 kOe for the sample annealed at 498 K. A quite similar behavior is also displayed by the other samples.

These peculiar optimizing features resemble those observed in magnetic nanowires and nanoparticle chains,[45] opening therefore the possibility to design specific devices for desired applications. Although the obtained field value, for a given temperature, at which the optimizing operating conditions occur may still not be the most interesting from the application viewpoint of micro- and nanomaterials, it is important however to keep in mind its relevance for future applications. Efforts in reducing the thermal hysteresis present in the magnetic transition by diminishing the glass coating thickness are in progress.

V. CONCLUSIONS

It has been shown the feasibility of producing a $Ni_{50}Mn_{34}In_{16}$ Heusler alloy with an off-stoichiometric composition in microwire shape geometry. Glass-coated microwires fabricated from this family of Ni-Mn-In Heusler alloys exhibit quite different magnetic properties from those for the bulk samples or ribbons of the same composition. The as-quenched microwire develops a highly ordered $L2_1$ cubic structure characteristic of the austenitic phase of Heusler alloys. It is maintained after short annealing treatments at 473 K and 498 K. $M(T)$ behavior is that of a typical ferromagnet for as-quenched and annealed microwires with almost the same Curie temperature around 246–248 K. Even in a low applied magnetic field of 50 Oe, FC curve retraces the ZFC one at a magnetization value corresponding to the demagnetizing limit for each sample, indicating no signature of structural transition. Magnetization does not saturate at the low temperature of 50 K here measured, and a splitting of the FC and ZFC due to AFM exchange is observed. It can also be detected when the *M(T)* measurements are performed at higher magnetic field in annealed microwires. Near T_C, a maximum entropy change around 1.75 J/kgK is achieved for both the as-quenched and the microwire annealed at 473 K at 30 kOe. Meanwhile, the largest value of maximum ΔS_M reaches 2.01 J/kgK for the microwire annealed at 498 K under a magnetic field change of 30 kOe. *RC* monotonously increases with the applied field for the three samples, reaching values even higher than 120 J/kg for applied fields around 30 kOe. Therefore, we observed a noticeable magnetocaloric effect and significant refrigerant capacity values making these microwires based on Heusler alloys very promising composites for multifunctional applications.

ACKNOWLEDGMENTS

Authors thank Professor M. Vazquez for providing fabrication of microwire samples at ICMM-CSIC. This work has been supported by Spanish MICINN Projects MAT2009-13108-C02-01 and 02, MAT2010-20798-C05-01 and 04. L. González and J. García acknowledge Spanish MICINN-FPI and FICyT-"Severo Ochoa" fellowships, respectively. D. Serantes thanks FICyT (Contract No. FC-10-COF10-04). The scientific support from the University of Oviedo SCT's is also acknowledged.

[1]V. Zhukova, M. Ipatov, and A. Zhukov, Sensors **9**, 9216 (2009).
[2]A. Labrador, C. Gomez-Polo, J. I. Perez-Landazabal, V. Zablotskii, I. Ederra, R. Gonzalo, G. Badini-Confalonieri, and M. Vazquez, Opt. Lett. **35**, 2161 (2010).
[3]F. Qin, V. V. Popov, and H.-X. Peng, J. Alloys Compd. **509**, 9508 (2011).
[4]T. T. P. Xuan, T. T. T. Le, P. D. Tran, B. V. Pham, D. H. Tong, and M. Ch. Dang, Adv. Nat. Sci.: Nanosci. Nanotechnol. **1**, 025013 (2010).
[5]S. M. Ueland and C. A. Schuh, Acta Mater. **60**, 282 (2012).
[6]M. Vazquez, H. Chiriac, A. Zhukov, L. Panina, and T. Uchiyama, Phys. Status Solidi A **208**, 493 (2011).
[7]K. Pirota, M. Hernandez-Velez, D. Navas, A. Zhukov, and M. Vazquez, Adv. Funct. Mater. **14**, 266 (2004).
[8]A. Zhukov, Adv. Funct. Mater. **16**, 675 (2006).
[9]M. I. Ilyn, V. Zhukova, J. D. Santos, M. L. Sanchez, V. M. Prida, B. Hernando, V. Larin, J. Gonzalez, A. M. Tishin, and A. Zhukov, Phys. Status Solidi A **205**, 1378 (2008).
[10]S. P. Farrell, P. E. Quigley, K. J. Avery, T. D. Hatchard, S. E. Flynn, and R. A. Dunlap, J. Phys. D.: Appl. Phys. **42**, 135005 (2009).
[11]C. Garcia, V. M. Prida, V. Vega, J. L. Sanchez-Llamazares, J. J. Suñol, Ll. Escoda, M. L. Sanchez, J. Ribot, and B. Hernando, Phys. Status Solidi A **206**, 644 (2009).
[12]Y. Chen, X. Zhang, D. C. Dunand, and C. A. Schuh, Appl. Phys. Lett. **95**, 171906 (2009).
[13]C. Gomez-Polo, J. I. Perez-Landazabal, V. Recarte, V. Sanchez-Alarcos, G. Badini-Confalonieri, and M. Vazquez, J. Appl. Phys. **107**, 123908 (2010).

[14]R. Varga, T. Ryba, Z. Vargova, K. Saksl, V. Zhukova, and A. Zhukov, Scr. Mater. **65**, 703 (2011).
[15]Y. Chen and C. A. Schuh, Acta Mater. **59**, 537 (2011).
[16]G. D. Liu, Z. H. Liu, X. F. Dai, S. Y. Yu, J. L. Chen, and G. H. Wu, Sci. Technol. Adv. Mater. **6**, 772 (2005).
[17]R. Kainuma, Y. Imano, W. Ito, Y. Sutou, H. Morito, S. Okamoto, O. Kitakami, K. Oikawa, A. Fujita, T. Kanomata, and K. Ishida, Nature **439**, 957 (2006).
[18]V. Srivastava, Y. Song, K. Bhatti, and R. D. James, Adv. Energy Mater. **1**, 97 (2011).
[19]T. Krenke, E. Duman, M. Acet, E. F. Wassermann, X. Moya, L. Mañosa, A. Planes, E. Suard, and B. Ouladdiaf, Phys. Rev. B **75**, 104414 (2007).
[20]A. K. Pathak, I. Dubenko, C. Pueblo, S. Stadler, and N. Ali, Appl. Phys. Lett. **96**, 172503 (2010).
[21]V. K. Sharma, M. K. Chattopadhyay, K. H. B. Shaeb, A. Chouhan, and S. B. Roy, Appl. Phys. Lett. **89**, 222509 (2006).
[22]A. K. Pathak, M. Khan, B. R. Gautam, S. Stadler, I. Dubenko, and N. Ali. J. Magn. Magn. Mater. **321**, 963 (2008).
[23]X. G. Zhao, C. C. Hsieh, J. H. Lai, X. J. Cheng, W. B. Cui, W. Lui, and Z. D. Zhang, Scr. Mater. **63**, 250 (2010).
[24]L. Mañosa, X. Moya, A. Planes, O. Gutfleisch, J. Lyubina, M. Barrio, J. L. Tamarit, S. Aksoy, T. Krenke, and M. Acet, Appl. Phys. Lett. **92**, 012515 (2008).
[25]L. Mañosa, D. Gonzalez-Alonso, A. Planes, E. Bonnot, M. Barrio, J. L. Tamarit, S. Aksoy, and M. Acet, Nature Mater. **9**, 478 (2010).
[26]Y. Sutou, Y. Imano, N. Koeda, T. Omori, R. Kainuma, K. Ishida, and K. Oikawa, Appl. Phys. Lett. **85**, 4358 (2004).
[27]I. D. Borisenko, V. V. Koledov, V. V. Khovailo, and V. G. Shavrov, J. Magn. Magn. Mater. **300**, e486 (2006).
[28]J. L. Sanchez-Llamazares, T. Sanchez, J. D. Santos, M. J. Perez, M. L. Sanchez, B. Hernando, Ll. Escoda, J. J. Suñol, and R. Varga, Appl. Phys. Lett. **92**, 012513 (2008).
[29]B. Hernando, J. L. Sanchez-Llamazares, V. M. Prida, D. Baldomir, D. Serantes, M. Ilyn, and J. Gonzalez, Appl. Phys. Lett. **94**, 222502 (2009).
[30]A. Planes, L. Mañosa, and M. Acet, J. Phys.: Condens. Matter **21**, 233201 (2009).
[31]A. M. Aliev, A. B. Batdalov, I. K. Kamilov, V. V. Koledov, V. G. Shavrov, V. D. Buchelnikov, J. Garcia, V. M. Prida, and B. Hernando, Appl. Phys. Lett. **97**, 2212505 (2010).
[32]D. C. Dunand and P. Müllner, Adv. Mater. **23**, 216 (2011).
[33]F. Qin, H.-X. Peng, J. Tang, and L.-C. Qin, Composites, Part A **41**, 1823 (2010).
[34]V. S. Larin, A. V. Torcunov, A. Zhukov, J. Gonzalez, M. Vazquez, and L. Panina, J. Magn. Magn. Mater. **249**, 39 (2002).
[35]T. Roisnel and J. Rodriguez-Carvajal, Mater. Sci. Forum **378–3**, 118 (2001).
[36]T. Krenke, M. Acet, E. F. Wassermann, X. Moya, L. Mañosa, and A. Planes, Phys. Rev. B **73**, 174413 (2006).
[37]S. Chatterjee, V. R. Singh, A. K. Deb, S. Giri, S. K. De, I. Dasgupta, and S. Majumdar, J. Magn. Magn. Mater. **322**, 102 (2010).
[38]L. González-Legarreta, T. Sánchez, W. O. Rosa, J. García, D. Serantes, R. Caballero-Flores, V. M. Prida, L. Escoda, J. J. Suñol, V. Koledov, and B. Hernando, J. Supercond. Novel Magn. (2012) (in press).
[39]C. García, A. Zhukov, J. González, V. Zhukova, R. Varga, J. J. del Val, V. Larin, and J. M. Blanco, J. Alloys Compd. **423**, 116 (2006).
[40]F. Rivadulla, J. Rivas, and J. B. Goodenough, Phys. Rev. B **70**, 172410 (2004).
[41]V. Franco and A. Conde, Int. J. Refrig. **33**, 465 (2010).
[42]H. Oesterreicher and F. T. Parker, J. Appl. Phys. **55**, 4334 (1984).
[43]V. M. Prida, V. Franco, V. Vega, J. L. Sánchez-Llamazares, J. J. Suñol, A. Conde, and B. Hernando, J. Alloys Compd. **509**, 190 (2011).
[44]N. H. Dung, Z. Q. Ou, L. Caron, L. Zhang, D. T. C. Thanh, G. A. de Wijs, R. A. de Groot, K. H. J. Buschow, and E. Brück, Adv. Energy Mater. **1**, 1215 (2011).
[45]D. Serantes, D. Baldomir, M. Pereiro, B. Hernando, V. M. Prida, J. L. Sanchez-Llamazares, A. Zhukov, M. Ilyn, and J. Gonzalez, Phys. Rev. B **80**, 134421 (2009).